

## The Modelling of the acquiring of „raw“ projection data in single-photon emission computed tomography

© M.A. Gurko, N.V. Denisova

Khristianovich Institute of Theoretical and Applied Mechanics SB RAS,  
630090 Novosibirsk, Russia  
e-mail: m.gurko@alumni.nsu.ru, nvdenisova2011@mail.ru

Received September 27, 2021

Revised November 29, 2021

Accepted December 11, 2021

The statistical modeling software package of the data acquisition at examining patients by single-photon emission computed tomography has been developed and tested. The modeling was performed by the Monte Carlo method and included the interaction effects of gamma radiation with matter under radiation transferring through biological tissues and through the collimator-detector system. The calculation of the gamma quanta transferring through the collimator has been verified by simulating clinical „syringe test“. Using the developed software package and the anthropomorphic mathematical model simulates a „virtual patient“, the acquisition of „raw“ projection data has been performed under conditions close to clinical practice. The images obtained are in agreement with clinical data.

**Keywords:** gamma radiation, collimator, Monte Carlo, modeling, phantom.

DOI: 10.21883/TP.2022.05.53682.264-21

### Introduction

State-of-the-art medical diagnostic equipment is characterized by complexity and variety of imaging techniques. In clinical practice, tomographic techniques such as X-ray computed tomography (CT), magnetic resonance imaging (MRI), positron emission tomography (PET) and single photon emission computed tomography (SPECT) are widely used. These techniques use various physical phenomena to detect pathological changes in biological tissues. CT and MRI methods are based on measuring physical characteristics of matter (density) in diseased and healthy tissues. Both methods have high resolution (around 1 mm), and image contrast is determined by difference in density in the diseased and healthy tissues. In the early stages of disease, density changes may be small and undetectable. Nuclear medicine PET and SPECT methods are based on using radiopharmaceuticals (RPs) containing nuclides that emit positrons and gamma rays in nuclear radioactive decay processes. In PET and SPECT tests a patient is administered an intravenous injection of a specialized radiopharmaceutical appropriate to the purpose of the test, which accumulates in varying concentrations in healthy and pathological tissues. PET and SPECT methods have lower resolution than CT and MRI methods (around 5 mm); however the contrast of images is not determined by the physical characteristics of tissues but rather by metabolic processes which determine different RP accumulation in healthy and diseased tissues. This makes it possible to diagnose pathological processes at an early stage, when there are still no changes in physical characteristics. For example, in SPECT examination of patients with cardiovascular diseases, methoxy-isobutyl-isonitrile (MIBI), tagged

with technetium is used, which is actively absorbed by healthy myocardial cells but does not enter the damaged cells. Such images have high contrast and are a marker of normal myocardial cell activity. FDG (fluorodeoxyglucose), which actively accumulates in tumors, is widely used in PET tests. Nuclear medicine techniques are widely used for diagnostics of cardiovascular diseases and cancers.

This paper considers SPECT technique. Despite the fact that SPECT is widely used in current clinical practice, there are unresolved problems related to improvement of image quality and optimization of the examination protocol. Recently there have been extensive studies aimed at developing a quantitative approach to assess the severity of damage in cardiology and oncology. Solving this problem requires a large number of tests. In nuclear medicine human studies are severely limited due to radiation exposure, and use of physical phantoms is complicated by high cost and low flexibility of their parameters. Therefore, the development of methods of mathematical modeling and computer simulations, which have proven themselves in other areas of modern physics, is relevant. Mathematical modeling of patient examination procedure by SPECT technique can be divided into three objectives:

- 1) creating a mathematical model of RP distribution in patient organs (virtual patient);
- 2) modeling of „raw“ data collection (virtual tomograph);
- 3) development of methods and algorithms for reconstruction of 3D-images.

The purpose of this paper is to simulate acquisition of „raw“ projection data in SPECT technique. Statistical modeling (Monte Carlo method) is used to solve this problem.

It should be noted that there are several off-the-shelf software solutions for calculating „raw“ PET and SPECT data. Most of them are open source and have well-developed documentation. One of the first suites is PENELOPE software suite written in FORTRAN 77. PENELOPE performs Monte Carlo simulations (MC) of electron-photon showers for a wide range of energies (from  $\sim 1$  keV to several hundred MeV) and has well-developed documentation describing physical processes of interaction between gamma rays and matter. Many software suites are rewritten in C++ and added to GEANT4 suite. PENELOPE is a universal tool, which is not specialized for nuclear medicine objectives, but finds its application in this area as well [1]. The next software suite, SimSET, designed, validated and supported by the University of Washington Imaging Research Laboratory, is designed to simulate SPECT and PET using voxel phantoms [2]. This suite applies MC methods to simulate physical processes and emission tomography devices. SimSET is a major resource for many nuclear medicine research groups around the world. SimSET simulates important physical phenomena including photoelectric absorption, Compton scattering, and coherent scattering. However, a collimator is not modeled by MC method, but using an approximate analytical model. This model does not account for some physical effects, such as gamma ray penetration through septum, characteristic emission, and scattering in a collimator. SimSET may be used as a good base for modeling gamma ray propagation through a patient's body. Recently, GATE software suite has become widely known. GATE is a set of MC modeling tools for medical physics applications [3]. It is based on GEANT4, a software suite designed in CERN (European Organization for Nuclear Research) for simulating passage of elementary particles through matter. GATE combines the advantages of GEANT4, well-tested physical models, sophisticated geometry description, powerful imaging and 3D-rendering tools with features specific to emission tomography. Using GATE does not require programming in C++ as it implements its own macro language. The entire source code is open. Precise and universal simulation codes such as GEANT3, EGS4, MCNP, and GEANT4, written for high-energy physics, include well-tested physics models, geometric modeling tools, and efficient imaging utilities [3]. However, their functionality is often redundant, and they are complex and time-consuming to learn and set up, so research groups often use their own „home-made“ developments.

Despite availability of ready-made solutions, such as PENELOPE, SimSET, GATE, to calculate „raw“ projection data, an independent solution can provide maximum flexibility for the requirements of a particular study. Therefore, in this paper, physical and mathematical modeling was performed and software was developed to calculate collection of „raw“ projection data in SPECT technique.

**Table 1.** Characteristics of SPECT isotopes

Isotope	Period of half-life, h	Energy gamma rays, keV	Probability emission gamma ray, %
Indium-111	67.32	171	90.5
		245	94
Technetium-99m	6.02	140	88.9
Iodine-123	13.22	159	82.8

## 1. Problem formulation. Physical and mathematical model

This paper investigates the problem of „raw“ data generation in SPECT technique. Projection data modeling actually involves three spatiotemporal problems:

- 1) modeling gamma ray emission during radioactive decay of the RP nuclide nuclei;
- 2) simulation of gamma ray passage in biological tissues of different densities;
- 3) simulation of gamma ray passage through collimator and detector material.

The emission process is modeled using anthropomorphic mathematical model of torso (MMT). This model describes RP distribution in the patient's organs and determines spatial characteristics of „source function“. This paper assumes that data acquisition time is significantly shorter than nuclide half-life as such, i.e., the time when local density of radioactive atoms decreases by a factor of two. This suggests that the average number of decays in each elementary volume remains approximately constant during data collection. Since there is no information on dedicated emission directions in radioactive decay, isotropy (equal probability) of emission directions is assumed. To describe passage of gamma rays through biological tissues and in the collimator–detector system, it is necessary to identify the main processes of interaction between gamma rays of certain energy and matter.

### 1.1. Characteristics of gamma rays in SPECT technique

Radiopharmaceuticals used in SPECT technique are sources of gamma rays with minimum percentage of alpha and beta emission. This effect is possible for isotopes with the presence of a long-lived excited state (isomerism of atomic nuclei).

Energy of nuclear gamma radiation is discrete, which is reflected in energy spectrum recorded by a gamma spectrometer by presence of one or more distinct peaks. Table 1 shows characteristics of three main SPECT isotopes.

This paper simulated data collection in process of examination of left ventricular myocardial perfusion in nuclear

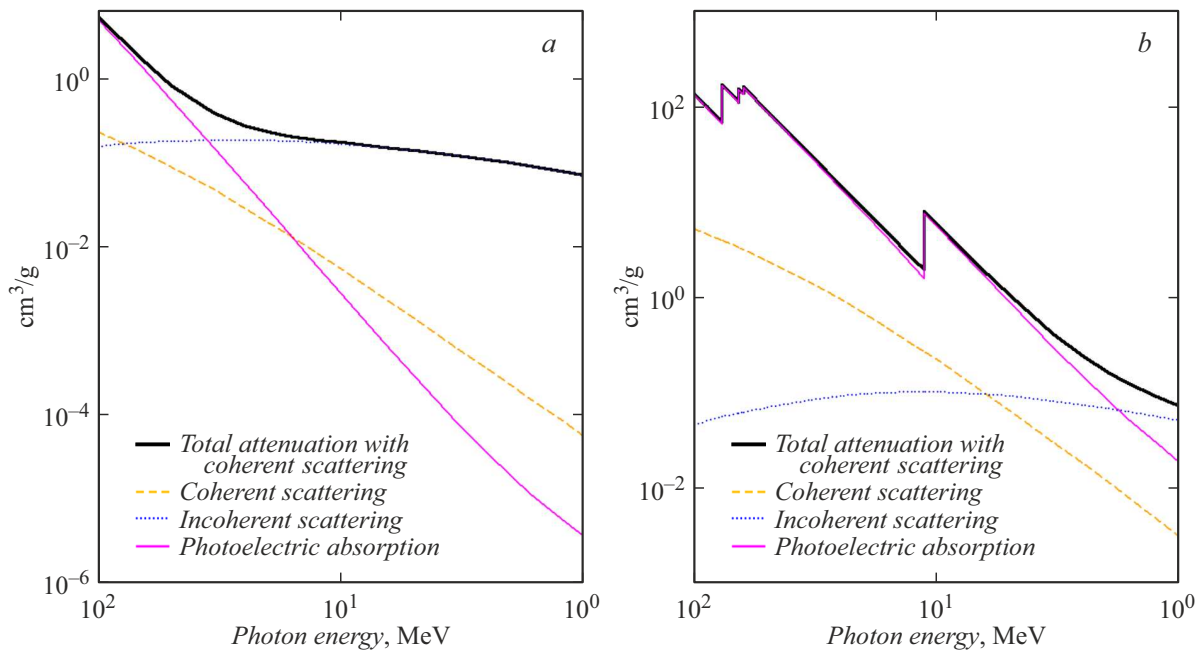


**Figure 1.** Energy dependence of mass attenuation coefficient of gamma radiation in water (a) and in lead (b).

cardiology using Tc99m-MIBI. As shown in the table, half-life of Tc99m is 6 h, and complete data collection time is usually 15–20 min.

## 1.2. Gamma radiation transfer in matter

As they propagate in matter, gamma rays are capable of experiencing various types of interactions [4,5]. They can be divided into two large classes: absorption and scattering.

In case of absorption, a gamma ray disappears, and its energy is transferred to matter or is spent to generate new particles. This class of interactions includes photoelectric effect (photoeffect), pair creation, and photonuclear absorption. But, because energies of gamma rays emitted by SPECT isotopes do not reach even 1 MeV, pair creation and photonuclear absorption are excluded.

In case of scattering, a gamma ray deflects from its original path at a certain angle, and part of its energy may be transferred to matter. This class includes coherent (Rayleigh) and incoherent (Compton) scattering. In coherent scattering, a gamma ray changes its path without changing the energy or internal state of the atom/molecule. Incoherent scattering is accompanied by a change in the path of gamma ray motion, its energy, and internal state of the atom (ionization).

For SPECT isotopes the main type of interaction of gamma rays with matter in biological tissues is incoherent scattering, and in a collimator and detector crystal — photoeffect. Dominance of photoeffect in the collimator and detector is a consequence and an important goal in their design, because photoeffect helps to achieve most effective absorption of gamma rays and, consequently, effective registration of their energy. Incoherent scattering

in biological tissues is a factor that can degrade quality of SPECT images. Firstly, negative effect of incoherent scattering is related to attenuation effect of photon flux. In state-of-the-art hybrid SPECT/CT systems, this effect is taken into account as an „attenuation correction “ by creating a so-called „attenuation map “ using low-dose CT. Secondly, negative effect of incoherent scattering is related to the fact that some of scattered photons, carrying false information about the trajectory, hit the detector (scatter effect). This phenomenon is compensated by means of energy discrimination, i.e. by introducing an energy window [6]. This makes it possible to cut off most of the scattered photons. Accounting of scattered photons arriving at the detector („scatter correction“) remains a challenging problem for current image reconstruction algorithms.

The basis for mathematical modeling of gamma ray propagation through matter is the law of radiation attenuation in matter:

$$N(x) = N_0 e^{-\tau x}. \quad (1)$$

Here  $\tau$  — linear attenuation coefficient, which determines probability of a gamma ray experiencing an interaction per unit of its path in a given matter.

Nuclear physics uses the mass attenuation coefficient, which is defined as the ratio of the linear attenuation coefficient to the density of matter:

$$\mu = \frac{\tau}{\rho} = \sigma \frac{N_A}{M}. \quad (2)$$

A view of the energy dependence of the mass attenuation coefficient in water and lead for the various effects is shown in fig. 1. These images were generated by NIST XCOM site for the given matters [6].

**Table 2.** Parameters of modeled collimators

Parameter of collimator	LEHR	LEAP	LEUHR	ME
Hole length, mm	24.05	24.05	35.8	40.64
Septal thickness, mm	0.16	0.2	0.13	1.14
Hole diameter, mm	1.11	0.2	1.16	2.94
Sensitivity*, cpm/ $\mu$ Ci	202	330	100	275
Geometric resolution*, mm	6.4	8.3	4.6	10.8
Septal penetration**, %	1.5	1.9	0.8	< 1.2

Note. \* — at distance of 10 cm, \*\* — for energy 140.5 keV.

As can be seen from these figures, Compton scattering of gamma rays plays a major role when gamma rays pass through biological tissues (water) with energies of around 140 keV. When passing through a crystal and a lead collimator, interaction of gamma rays with matter is determined by dominant photoeffect.

Angular distribution of scattered gamma rays is described by a scattering angle indicatrix. Functions used to model the scattering angle indicatrix are always approximating functions. The problems of the exact representation of the indicatrix for coherent and incoherent scattering are described in the literature [7].

## 2. Method for solving the problem posed

In this study, MC method was applied as capable of solving this kind of problem as correctly as possible. There are many numerical algorithms using MC to study various random processes. Nowadays, practically any studies of physical processes will not go without using MC method. The substance of this method is the application of a set of independent output data based on random variables, followed by their averaging to obtain the probabilities of a certain result.

In the field of nuclear medicine, MC has found its niche as a reference method for modeling „raw“ data collection [2,3]. In this study, the basis for process of modeling gamma ray propagation in matter is a combination of several methods. The first method solves the problem of finding the first intersection of the gamma ray trajectory with the nearest interaction object. By the nature of the problem to be solved, this method can be called the ray shooting method, which is known in the English literature as ray casting [9]. The second method — is the maximum cross-section method (in the English literature Woodcock tracking), which makes it possible to provide fast and algorithmically simple simulation of gamma ray propagation in a complex environment [8,10–12]. This method is very convenient when the complex environment is represented as a three-dimensional array of attenuation coefficient values. Also in this study, the Woodcock tracking method was applied to simulate gamma ray propagation in a collimator.

An important and not the easiest task is modeling of gamma ray scattering angle indicatrix. The most common method used to solve this problem is the exclusion method [8]. In this study, incoherent scattering angle indicatrix was modeled using the Klein–Nishina–Tamm [5] exclusion formula. An adapted GEANT4 module called G4RayleighAngularGenerator, which is also based on the exclusion method, was used to simulate the coherent scattering angle indicatrix.

It is convenient to use the inverse function [8,10,11] method to simulate discrete random variable distribution. This method was used when modeling distribution of the interaction type, in other words, to select the type of interaction at the interaction point. When the number of possible values of a discrete random variable is large, it is reasonable to use the Walker method [10]. In this study it was used to model distribution of gamma ray emission coordinates.

## 3. Numerical experiments aimed at calculation of collimator and crystal specifications

The first series of numerical experiments studied the effect of collimator and crystal specifications on SPECT images. The study was performed using a gamma ray point source with energy of 140.5 keV. The 4 types of collimators used in the Siemens Symbia T Series were compared. The parameters of the selected collimators are shown in table 2. The other simulation parameters, such as specifications of the detector crystal and its geometrical dimensions, the distance from the source to the collimator surface (gamma-camera) were the same for all experiments.

Here and below the common abbreviations are used:

- LEHR — Low Energy High Resolution
- LEAP — Low Energy All Purpose
- LEUHR — Low Energy Ultra High Resolution
- ME — Medium Energy.

The stated sensitivity and resolution were determined according to NEMA NU-1 2007 standard for a 9.5 mm thick crystal.

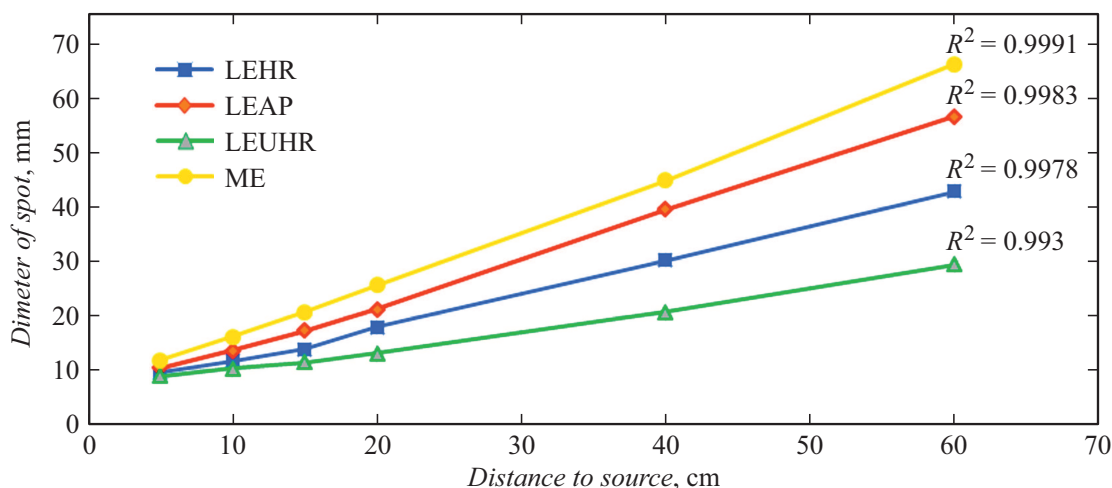


**Figure 2.** Dependence of spot size on distance to point source.  $R^2$  — validity ratio of linear approximation.

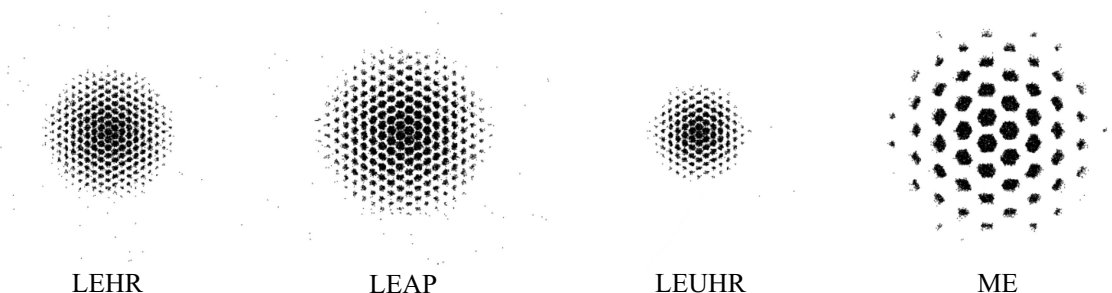


**Figure 3.** Point source images for different collimators at distance of 20 cm.

The syringe test mode, which is a regular test procedure for clinical SPECT tomographs, was simulated. This test is a control test for point source response. The simulated acquisition time was 10 s and the point source activity was 70 MBq. Spot size was defined as the total width at 10% of the height of intensity distribution maximum in the spot. Dependence of the spot size on the distance to the point source is shown in fig. 2.

Fig. 3 shows the spots from the point source at a distance of 20 cm for the studied collimators. Scattering acts are excluded from the spot image, and the spatial resolution of the detection system is assumed to be 0.1 mm. There is no intensity gradient, i.e., the pixel color reflects the fact of gamma ray registration, not the intensity of registration. Thus, these images include two components: a geometric component and a component corresponding to the penetration of gamma rays through the collimator walls. These images are intended to demonstrate the collimator operation.

The second series of experiments was performed using the anthropomorphic MMT phantom. This phantom has been developed in Institute of Theoretical and Applied Mechanics, Siberian Branch of Russian Academy of Sciences, and is based on equations of analytical geometry, which provides flexibility in modeling the in-

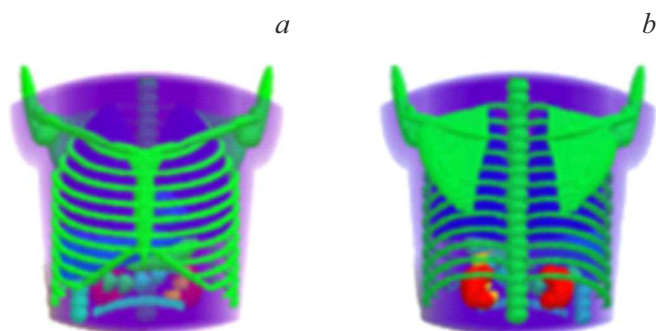


**Figure 4.** 3D-phantom MMT with front (a) and rear (b) sides.

dividual anatomical features of the patients. Fig. 4 shows the frontal and posterior views of a MMT phantom.

For numerical experiments, the spatial arrangement of the source function and rotating gamma-camera were modeled to approximate the characteristics of clinical SPECT systems. To demonstrate geometry of the simulation process, a three-dimensional distribution of absorbed energy in the simulation space with the frontal projection build-up of the MMT phantom is shown in fig. 5.

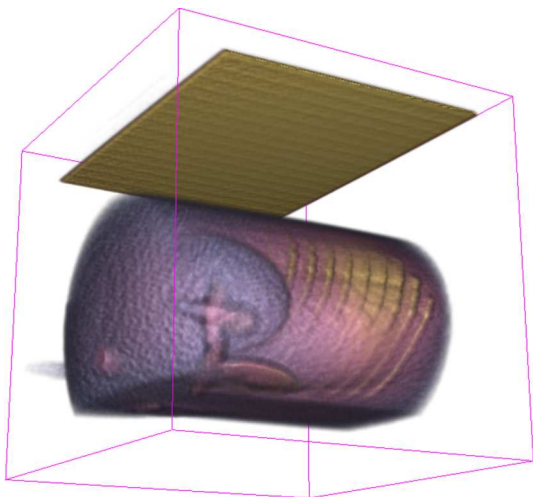


**Figure 5.** Three-dimensional distribution of absorbed energy in simulation space.

The simulation space in fig. 5 is a cube with a human body phantom and gamma-camera placed therein. The human body phantom performs two roles:

- 1) source function — spatial probability distribution of gamma ray emission;
- 2) attenuation map — spatial distribution of materials for which the attenuation coefficient is calculated during simulation.

To investigate the effect of collimator parameters on SPECT images, a 25-s build-up of four frontal projections of an MMT phantom with an introduced activity of 300 MBq at 10 cm from the gamma-camera was simulated. In this case, the system parameters are approximated to the real ones. NaI(Tl) scintillator with thickness of 0.95 cm was simulated. The geometrical resolution of the detector crystal was adopted to be 4 mm, scattering acts were taken into account, decay time was 300 ns, and energy resolution was 9.9%. The resulting projections are shown in fig. 6.

The number of gamma rays registered for a fixed projection build-up time makes it possible to estimate collimator sensitivity. For a rough estimation the ratio of the number

of registered gamma rays was used, where the number of registered gamma rays for a LEAP collimator was taken as a unit. The results obtained are presented in table 3.

## 4. Numerical experiments approximated to clinical practice

The following series of numerical experiments were performed using an anthropomorphic mathematical phantom (virtual patient). In these experiments the data collection procedure was simulated for myocardial perfusion examination by SPECT/CT using a radiopharmaceutical Tc-99 MIBI.

### 4.1. Phantom description

The MMT phantom was used to simulate distribution of radiopharmaceutical  $^{99m}\text{Tc}$ -MIBI, which is used in nuclear cardiology to diagnose myocardial perfusion disorders [13]. A view of this phantom is shown in fig. 7, a.

In clinical studies, values of RP concentrations in various organs may vary from patient to patient. Table 4 shows the relative radiopharmaceutical concentration values used in this study, which were selected taking into account the clinical results provided by the radionuclide diagnostic department of the M.I. Miasnikov Institute of Cardiology.

Based on the MMT phantom, a 3D attenuation map was generated. This map is a 3D-matrix of material indices, which are used to calculate linear attenuation coefficients in the simulation process. Three types of material in the phantom were distinguished: air (lungs), water (soft tissues), and bone tissue. Data on material compositions were taken from ICRU-44 [14] report. Attenuation coefficients for these materials were calculated by interpolation of tables based on NIST XCOM [15]. B-100 Bone-Equivalent Plastic was used to calculate the attenuation coefficient for bone structures; lungs were modeled as Lung Tissue with a density equal to that of air. A view of the attenuation map based on the MMT phantom is shown in fig. 7, b.

Fig 8 presents comparison of „CT slices“ of MMT phantom with clinical data. An imaging window is a linear gradient of color from minimum value of attenuation

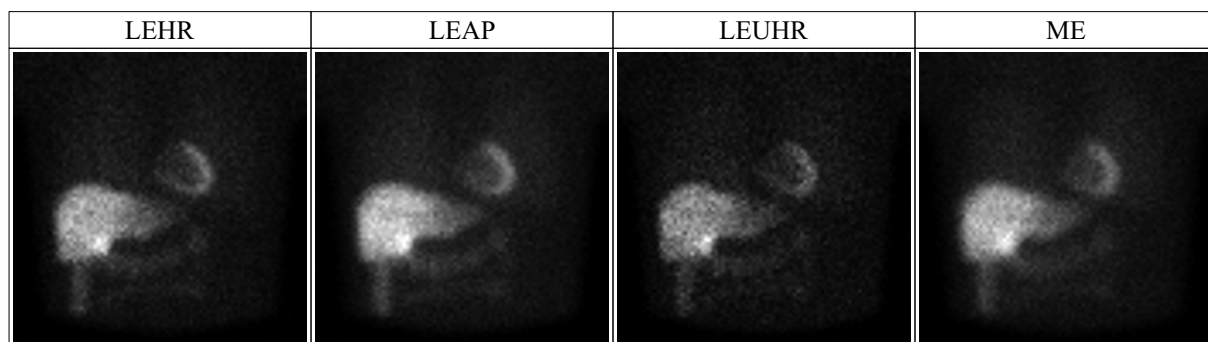


**Figure 6.** 25-second frontal projections of MMT phantom.



**Table 3.** Sensitivity of collimators

Data on sensitivity	LEHR	LEAP	LEUHR	ME
Number of registered gamma rays for frontal projections	229878	392837	117828	353381
Number of registered gamma rays for point source*	18793	32831	9828	29366
Relative sensitivity for frontal projections	0.59	1	0.3	0.89
Relative sensitivity for point source*	0.57	1	0.3	0.89
Stated relative sensitivity*	0.61	1	0.3	0.83

Note. \* — at distance of 10 cm.

**Table 4.** Relative concentration value of radiopharmaceuticals

Organ	Relative RP concentration
Soft tissues	~ 1.3
Lungs	1
Left ventricle of heart	~ 20
Liver	~ 20
Intestinal tract	14.5–40
Gallbladder	~ 50

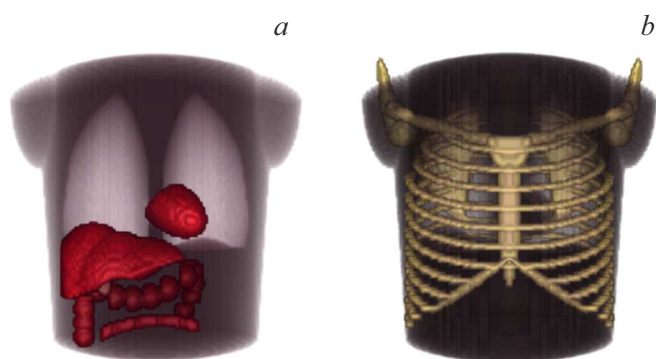


**Figure 7.** 3D-source function (a) and attenuation map (b), generated based on MMT phantom.

coefficient (air), corresponding to black color, to maximum (bone tissue) — white color. Such style of imaging window is fair for all images presented in this paper.

#### 4.2. Description of experiment conditions

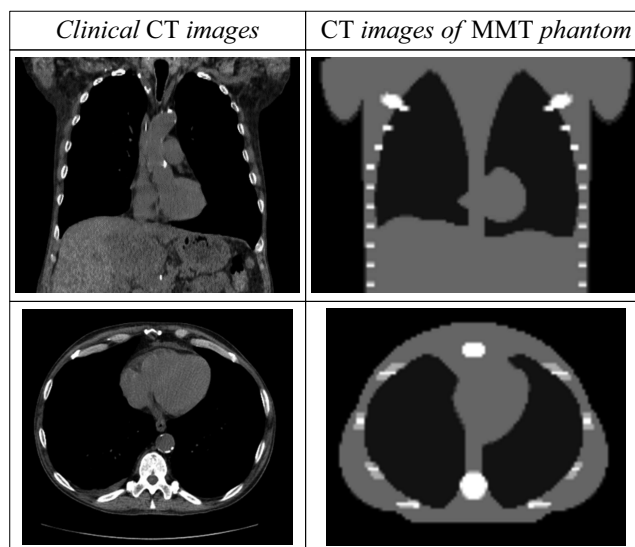
Comparison of „raw“ data obtained by simulation to clinical results makes it possible to verify methods and approaches to calculation of „raw“ data. To this end, projection data was calculated using a virtual patient (MMT phantom) and a virtual tomograph (MC simulation). Numerical experiment conditions were approximated to clinical practice. A virtual patient was placed in a virtual tomograph using a gamma-camera with LEHR-collimator

(table 2). A circular orbit of the gamma-camera with a radius of 25.6 cm was simulated. The projection build-up angle relative to the frontal ( $0^\circ$ ) varied from  $-135^\circ$  (left posterior oblique) to  $45^\circ$  (right anterior oblique). In the frontal projection, the distance from the patient's body to the collimator was approximately 15.6 cm. 32 projections were built up with a fixed acquisition time. The acquisition time for each projection was 15 s. All the simulation parameters are presented in detail in table 5.

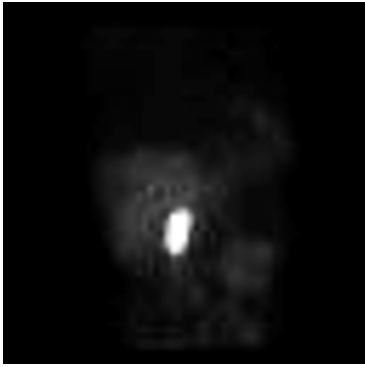
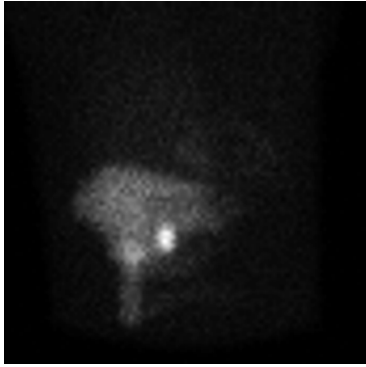
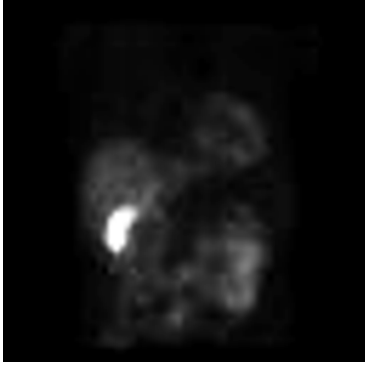
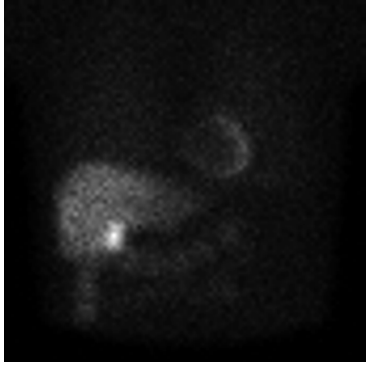
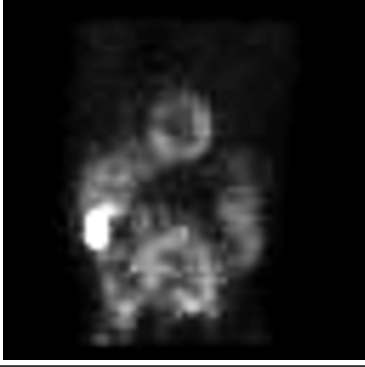
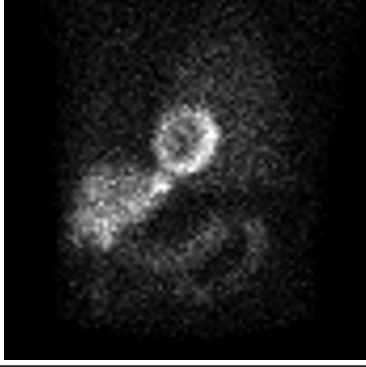
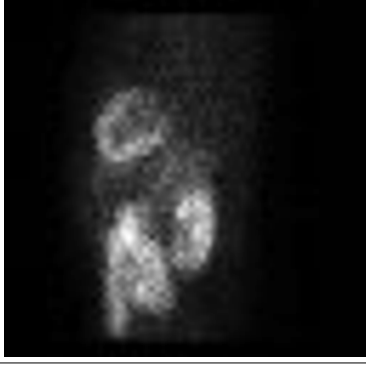
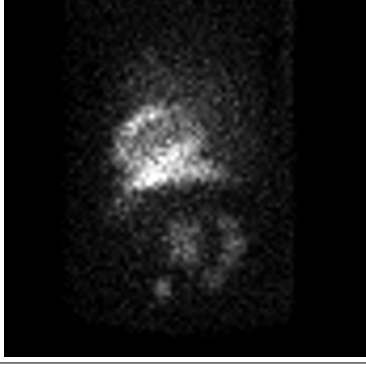
#### 4.3. Results of the numerical experiment

Numerical simulations produced planar images for 32 gamma-camera rotation angles. To demonstrate a comparison with clinical planar images, 4 projections were chosen. In clinical practice of nuclear cardiology, 4 standard projections (views) are used to demonstrate the result: right anterior oblique ( $45^\circ$ ), anterior ( $0^\circ$ ), left anterior oblique ( $-45^\circ$ ) and left lateral ( $-90^\circ$ ).

The comparison was made with the data provided by the E. N. Meshalkin National Medical Research Center. The view of the four projections is shown in fig. 9.



**Figure 8.** Comparison of „CT slices“ of MMT phantom with clinical data.

<i>View</i>	<i>Clinical results</i>	<i>Obtained results</i>
<i>Right anterior oblique</i>		
<i>Anterior</i>		
<i>Left anterior oblique</i>		
<i>Left lateral</i>		

**Figure 9.** Comparison of produced results with clinical ones.

## Conclusion

A collimator is an important device in a gamma-camera, which determines the quality of produced „raw“ data,

and in the end, quality of resulting SPECT images. The performed studies have shown that the dependence of spot size on the distance to the point source, shown in fig. 2, has a linear nature, which coincides with the theoretical



**Table 5.** Values of modeling parameters

Modeling parameter	Parameter value
Patient	MMT Phantom (table 2)
Introduced activity	300 MBq
Number of projections	32
Angle of projection (relative to frontal projection)	–135–45°
Time of projection build-up	10 s
Collimator	LEHR (table 2)
Orbit radius	25.6 cm
Detector material	NaI
Detector thickness	0.95 cm
Detector decay time	300 ns
Detector energy resolution	9.9%
Detector spatial resolution (FWHM)	0.4 cm

calculations [4,13]. The angular coefficient of these lines is of particular interest. It can be seen that the collimator distance has the least influence on the resolution for the LEUHR collimator. At the same time, the ME collimator, judging from this relationship, has the largest difference between the resolution for near and far layers of the patient's body, which is important to keep in mind during examination. The results shown in fig. 3 are consistent with the images obtained using analytical formulae within the Fourier decomposition [16]. By the wall thickness of the aortic ventricle in fig. 6 we can determine the geometric resolution of the collimators. The best result was given by LEUHR collimator. From the obtained projections we can also see that in case of the LEUHR collimator it takes more time to build up images with good statistics. A good agreement of the collimator sensitivity values obtained from the simulation with those stated by the manufacturer is observed in table 3. Therefore, the results of calculations of the gamma ray transfer through the collimator performed in this paper by MC method are consistent with the calculations performed by other methods, with the measurement data, and with the characteristics declared by the manufacturers.

Fig. 9 shows comparison of clinical planar images with the images obtained in the present paper. It should be noted that the location and size of the organs, the ratio of the accumulated activities depend on the individual anatomical features of the patient, as well as the time of the examination relative to the moment of the drug injection. All these parameters may vary, so it is difficult to make quantitative comparisons. Visual comparison shows good consistency in size and relative location of liver and aortic ventricle. Therefore, the results of calculations of „raw“ projection data performed in this paper by MC method, are

consistent with clinical images and may be used to model data collection procedure in SPECT /CT method.

## Conclusions

A software suite based on MC method has been designed to simulate the patient examination procedure by SPECT/CT (virtual tomograph). This approach allows to collect „raw“ data approximating clinical results. Since the inverse problem solution uses a system matrix based on the analytical approach, the application of MC method to solve the actual problem provides solution independence, which is an important factor in the numerical simulation of the patient examination procedure. Besides, this software solution can be modified for other tasks of nuclear medicine, for example, for simulation of the patient examination procedure by the PET method.

Calculation of gamma rays passage through a collimator was implemented, tested and verified. Calculation of projection images was approximated as much as possible to the actual clinical procedure. Good consistency with the clinical results was obtained. This makes it possible to discuss successful verification of calculations of gamma radiation passage in biological tissues and through the collimator–detector system.

## Acknowledgments

We would like to thank S.M. Prigarin for his assistance in implementation of MC method algorithms.

## Funding

The research was carried out with support granted from the Russian Foundation for Fundamental Research №19-02-00244-A.

## Conflict of interest

The authors declare that they have no conflict of interest.

## References

- [1] L.M. Rodríguez. *Phys. Med. Biol.*, **53** (17), 4573 (2008).
- [2] R. Harrison. *AIP Conf. Proc.*, **1204**, 126 (2010).
- [3] S. Jan, G. Santin, D. Strul, S. Staelens, K. Assié, D. Autret, S. Avner, R. Barbier, M. Bardiés, P.M. Bloomfield, D. Brasse, V. Breton, P. Bruyndonckx, I. Buvat, A.F. Chatzioannou, Y. Choi, Y.H. Chung, C. Comtat, D. Donnarie. *Phys. Med. Biol.*, **49** (19), 4543 (2004).
- [4] V.A. Klimanov. *Fizika yadernoy meditsiny*, (Natsionalny issledovatel'skiy yaderny universitet „MIFI“, M., 2012), ch. 1. (in Russian)
- [5] V.I. Bepalov. *Vzaimodeystvie ioniziruyushchego izlucheniya s veschestvom* (Izd-vo Tomskogo politekh. un-ta, Tomsk, 2008) (in Russian)
- [6] National Institute of Standards and Technology, „NIST XCOM: Element/Compound/Mixture“. Available: <https://physics.nist.gov/PhysRefData/Xcom/html/xcom1.html>
- [7] J.H. Hubbell, W.J. Veigele, E.A. Briggs, R.T. Brown, D.T. Cromer, R.J. Howerton. *J. Phys. Chem. Reference Data*, **4** (3), 471 (1975).
- [8] G.A. Mikhailov, A.V. Voytishchek. *Statisticheskoe modelirovanie. Metody Monte-Karlo: uchebnoe posobie dlya bakalavriata i magistratury* (Izd-vo Yurayt, M., 2018) (in Russian)
- [9] J.D. Foley, A. van Dam, S.K. Feiner, J. Hughes. *Computer Graphics: Principles and Practice* (Addison-Wesley, USA, 1995)
- [10] S.M. Prigagin. *Osnovy statisticheskogo modelirovaniya perenosa polarizovannogo opticheskogo izlucheniya: uchebnoe posobie* (Novosib. gos. un-t., 2010)
- [11] I.M. Sobol. *Chislennyye metody Monte-Karlo* (Nauka, M., 1973) (in Russian)
- [12] E.R. Woodcock, J.T. Murphy, P. Hemmings, S.C. Longworth. *Techniques Used in the GEM Code for Monte Carlo Neutronics Calculations in Reactors and Other Systems of Complex Geometry*. *Proceed. Conf. Application of Computing Methods to Reactor Problems*, p. 557, 1965.
- [13] A.A. Ansheles, V.B. Sergienko. *Yadernaya kardiologiya* (FGBU „NMITs kardiologii“ Minzdrava Rossii, M., 2021)
- [14] *Tissue Substitutes in Radiation Dosimetry and Measurement* (International Commission on Radiation Units and Measurements, 1989)
- [15] M.J. Berger, J.H. Hubbell, S.M. Seltzer, J.S. Coursey, C.J. Chang, R. Sukumar, D.S. Zucker, K. Olsen. *XCOM-Photon Cross Sections Database, NIST Standard Reference Database 8 (XGAM)*. 1987. <https://www.nist.gov/pml/xcom-photon-cross-sections-database>
- [16] A.R. Formiconi. *Phys. Med. Biol.*, **43** (11), 3359 (1998).